Supplement of Earth Syst. Dynam., 7, 203–210, 2016
http://www.earth-syst-dynam.net/7/203/2016/
doi:10.5194/esd-7-203-2016-supplement

Supplement of

Delaying future sea-level rise by storing water in Antarctica

K. Frieler et al.

Correspondence to: A. Levermann (anders.levermann@pik-potsdam.de)

S1 Efforts of delaying sea level rise in comparison to local adaptation

Storing ocean water 700km inland on the Antarctic Ice Sheet requires overcoming a height difference of about 4000m. Mitigating a sea-level rise of 3 mm yr-1 requires 1275 GW of power to increase the potential energy of the water accordingly. This corresponds to a power of 10 kW that is required to pump 1 m^3/s vertically to a height of 1m. The actual energy required for the pumping will be higher due to friction and inefficient pumping. Here we assume a required power of 18 kW to pump 1 m^3/s to a height of 1m. This value is based on the project Tagus-Segura Water Transfer(Melgarejo Moreno, Joaquín Sanz Montaño, 2009). In its first section (TRAMO I) a power of 135 MW is applied to achieve a through-put of 31.7 m^3/s over a height difference of 245 m, which corresponds to 17.3 kW/(m^3/s)/m. This would mean that the required power to mitigate a sea-level rise of 3 mm yr-1 would reach about 2300 GW. To avoid further greenhouse-gas emissions the power would have to be generated based on local renewable technologies.

That poses a fundamental engineering problem that goes far beyond the scope of existing projects. While wind power plants and pipeline technology readily exist, currently the required technology is not available for the very low temperatures of Antarctica, as far as we know. We cannot provide reliable estimates of the associated costs at this stage.

However, to put the engineering effort into perspective we here compare the technical requirements of the pumping and transporting system to that of the Trans Alaska Pipeline (TAP)(Alyeska Pipeline Service Company, 2013). Thereby we assume that the transport of the water is split up into 90 individual pipelines each ensuring a throughput of $11\cdot10^9$ m^3 yr^{-1} as provided by the largest New Orleans pumping station.

	Trans Alaska Pipeline	**Individual pipeline of the potential Antarctic pumping system**
Length	1287 km	700 km
Maximum elevation	1444 m	4000 m
Air temperature along route	-60°C to 35°C	far below 0°C
Annual throughput	$0.1245 \cdot 10^9$ m^3 (assuming a maximum daily throughput as reached in 1988)	$11 \cdot 10^9$ m^3

The costs of building the TAP amount to a total of 8 billion US$. On the one hand this includes costs not relevant for the Antarctic pipelines and pumps such as:

- costs of the Valdez oil terminal (US$1.4)
- launching/receiving facilities for cleaning pigs that sweep the pipe of built-up wax, water or other solids that precipitate out of the oil stream
- 124,300 heat pipes along the pipeline transferring ground heat into the air during cold periods to lower the ground temperature to ensure that soils remain frozen throughout the summer to steadily support the pipeline (to be replaced by alternatives adequate for Antarctica).

While on the other hand the Antarctic systems will

- have to provide an orders of magnitude higher throughput (assuming 90 individual lines starting at the ocean with an annual throughput of $11 \cdot 10^9$ m^3 as provided by the largest New Orleans pump station would require an upscaling of the maximum annual throughput of the TAP (calculated based on its maximum daily throughput reached in 1988) by a factor of 90 for each individual line).
- have to overcome a larger elevation difference (4000m in comparison to a maximum of 1444 m along the TAP)
- require heating along the pipelines

- require a system to distribute the water on the ice sheet
- need an adjustments of the pipeline due to moving ice

to provide a simplistic upscaling of the TAP costs excluding the terminal (6.6 US$) to the required length (L), height (H), and capacity (P) we assume that the overall costs C can be split up in to components, a first one C_1 that scales with P and H (mainly representing the costs of the pump stations) and a second one C_2 that scales with L and P (mainly representing the costs of the pipeline itself). Assume that the two components of the overall costs of the TAB C_{TAB} are given by $C_{1,TAP} = \alpha C_{TAP}$ and accordingly $C_{2,TAP} = (1-\alpha)\ C_{TAP}$ that would mean that

$$\mathrm{C} = C_{1,TAB} * \frac{P}{P_{TAB}} * \frac{H}{H_{TAB}} + C_{2,TAB} * \frac{P}{P_{TAB}} * \frac{L}{L_{TAB}}$$

$$\approx \alpha\, 6.6 * 10^{12}\, US\$ * 8015 * 3 + (1-\alpha)\, 6.6 * 10^{12}\, US\$ * 8015 * 50$$

with C = 158,697 billion US$ for $\alpha = 1$ and C = 2,644,950 billion US$ for $\alpha = 0$. Both numbers do not include the costs of running and maintaining the system. Assuming they are minor compared to the cost of construction, construction costs could be divided by 100 to estimate the annual costs over the 21st century. In both cases they are orders of magnitude higher than the estimated annual investment and maintenance costs of local adaptation by dikes of US$ 12–71 billion in 2100(Hinkel et al., 2014) which however only protects regions that are economically expendient to protect. This might exclude for example the AOSIS small island states and their culture as well as UNESCO cultural heritage sites(Marzeion and Levermann, 2014).

That means that such a project would only become competitive with major efficiency gains by technical innovations and learning from the experience of the project itself.

S2 Wind Energy potential in Antarctica

We follow the methodology of ref. (Archer and Jacobson, 2005) to estimate the wind energy that is available in a 200 km wide band along the East Antarctic coast (Fig. S1). We use the yearly mean wind data for 2014 at 10m above the surface from the Era-Interim dataset(ECMWF, n.d.). Following ref. (Archer and Jacobson, 2005), we use only regions with average wind speed above 6.5 m/s. The power of a single wind turbine can be estimated by (ref. (Archer and Jacobson, 2005), equ. 19):

$$\mathrm{P} = P_{rated} * \mathrm{CF} = P_{rated} * (0.087V - \frac{P_{rated}}{D^2})$$

with P as average power output, P_{rated} the rated power of a single wind turbine, CF the conversion factor, V the average yearly wind speed and D the rotor diameter of the wind turbine. Six wind turbines of the 1.5 MW class can be installed per square kilometre(Archer and Jacobson, 2005). Integrating over the East Antarctic band area with wind stronger than 6.5 m/s, we estimate a wind power potential of 16.7 TW. Regions difficult to access, such as mountain ranges, and regions of fast flowing ice have not been excluded from the total area. We do not apply a conversion of 10m above-surface winds to such at the height of the rotor (80m in ref. (Archer and Jacobson, 2005)). As winds at 80m are generally higher than at 10m above the surface, the real wind energy potential may be higher.

Wind power utilization in Antarctica will pose a number of major challenges that cannot be addressed here. These include building fundaments on moving and deformable ground, functioning under extremely cold temperatures in Antarctic winters and handling very high wind velocities.

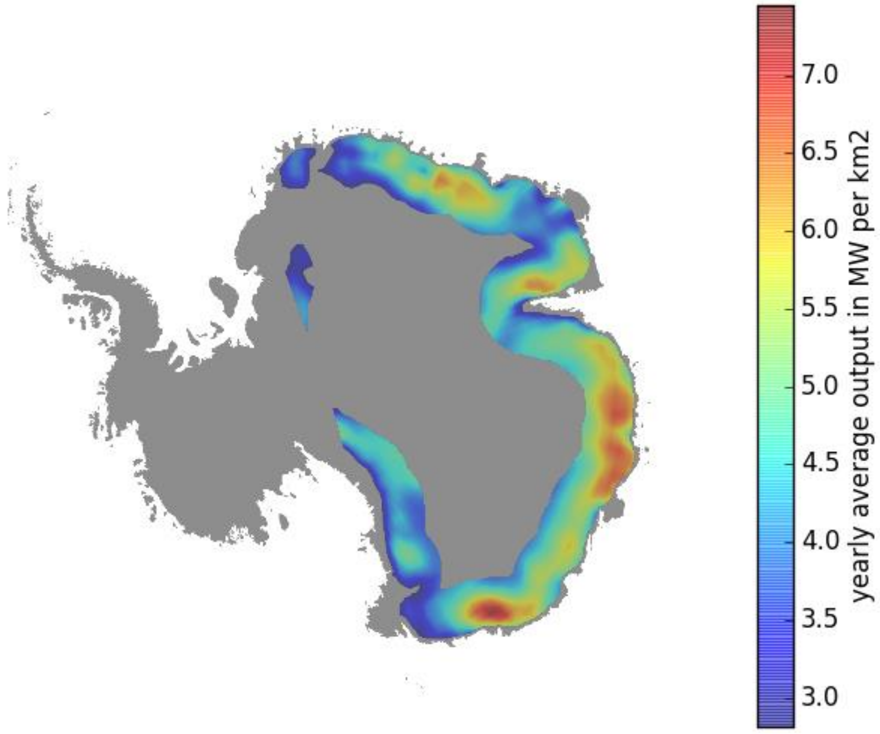

Fig. S1: Wind energy potential in East Antarctica. Using ERA-Interim data(ECMWF, n.d.), we use the methodology of ref. (Archer and Jacobson, 2005) to estimate the wind power potential in a 200km-wide strip along the East Antarctic coast. High wind speeds above 6.5 m/s on yearly average in the major part of the strip allow for large-scale wind energy extraction.

S3 Modelled initial equilibrium ice sheet state

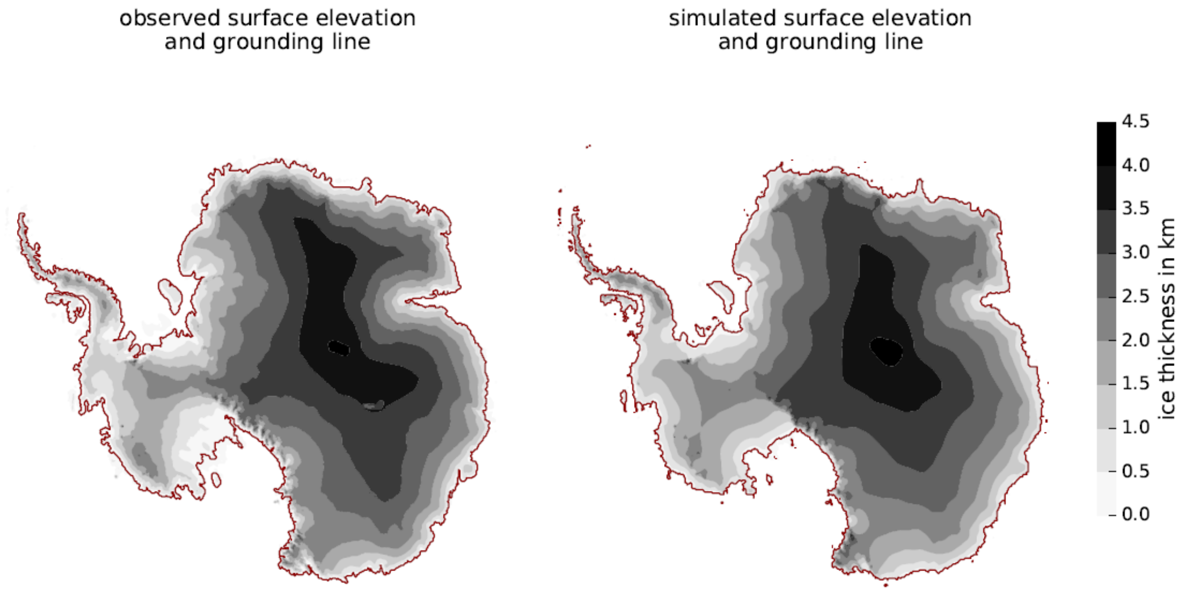

Fig. S2: Comparison of the currently observed surface elevation and grounding line position (left panel) to the simulated initial state of the ice sheet (right panel). The grounding line (red line, Bindschadler et al., 2011) is generally well reproduced for East Antarctica and most parts of West Antarctica. East Antarctica's modelled surface elevation compares well to the observed state (Fretwell et al., 2013). The modelled surface elevation is slightly higher close to the South pole and slightly lower towards the East Antarctic coast as compared the observation.

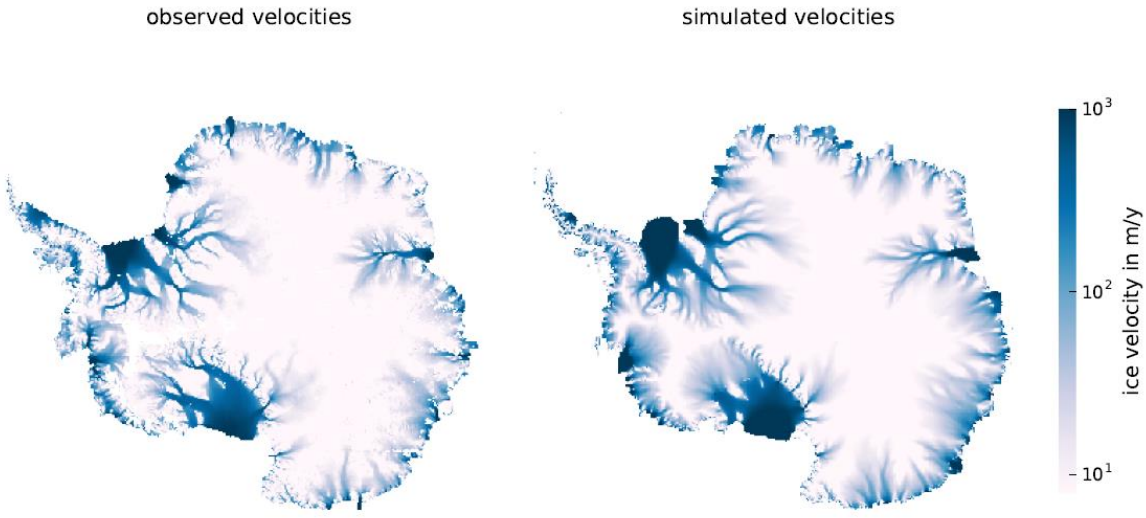

Fig. S4: Comparison of the currently observed ice velocities at the surface (left panel, Rignot et al., 2011) to the velocities of the simulated initial state of the ice sheet (right panel). The model reproduces the flow features of the East Antarctic ice sheet.

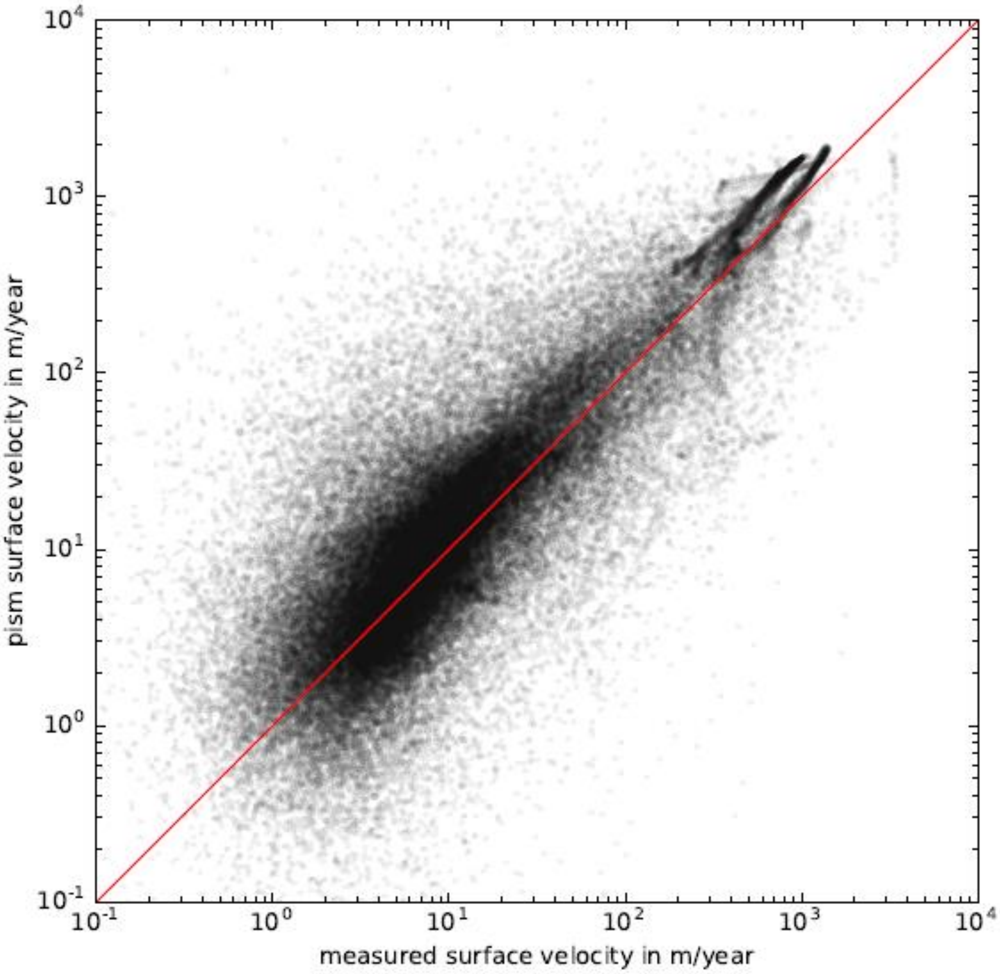

Fig. S5: Observed and modelled velocities, point-to-point comparison on log-log scale. Observed velocities (Rignot et al., 2011) are on the x-axis and modelled velocities on the y-axis.

S4 Long term response

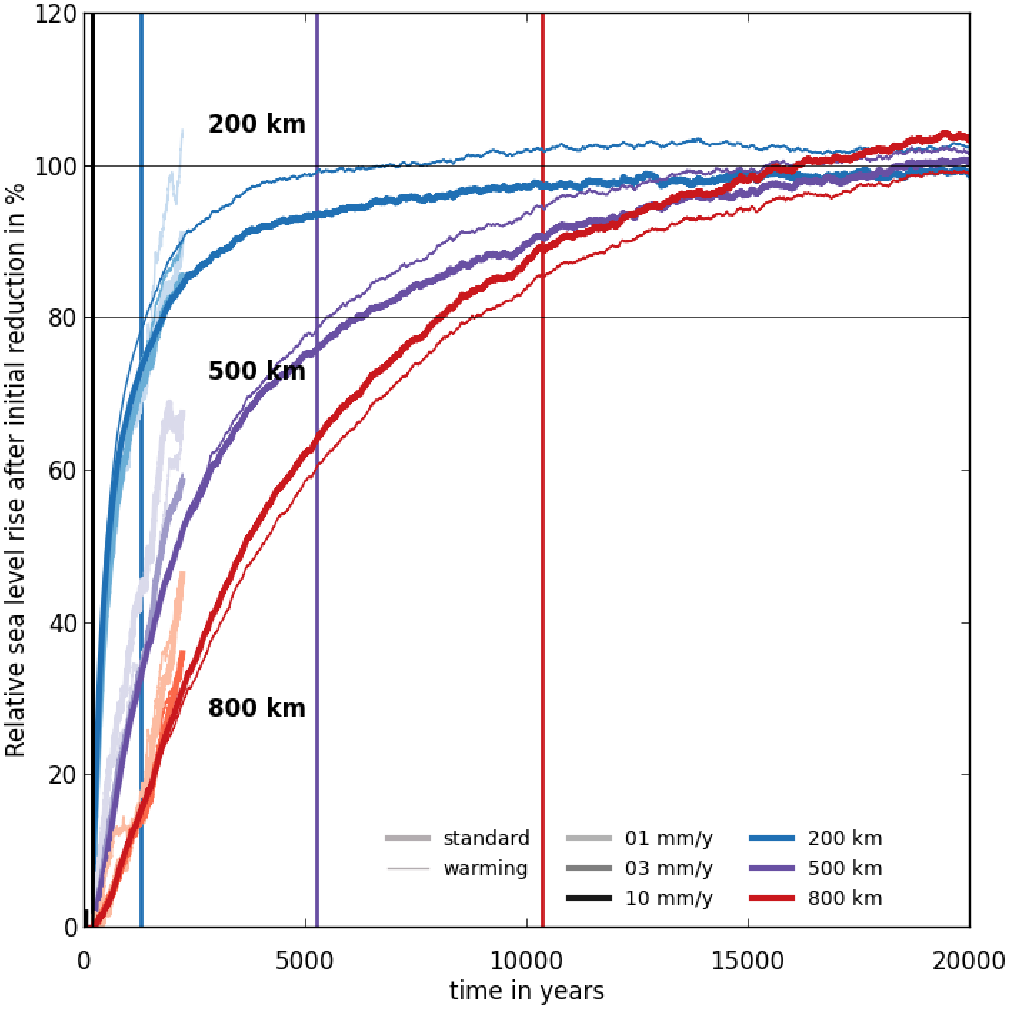

Fig. S5: Delayed sea-level rise as fraction of the initial reduction. Colour coding indicates the application band where the ice is added (red: 800 km distance from the coast, violet: 500 km distance from the coast, and blue: 200 km distance from the coast). The colour intensity describes the application rate from 1mm yr^{-1} (light), via 3 mm yr^{-1} (normal) to 10 mm yr^{-1} (dark). Thin lines show the results of the simulations accounting for latent-heat release while thick lines represent the results without the additional warming. Vertical lines mark the 5th percentile of the distribution of delay times assuming an ice parcel traveling 800 km (red), 500 km (violet), and 200 km (blue) with a constant surface velocity drawn from the distribution of surface velocities observed within the area of less than 800 km, 500 km and 200 km distance from the coast. Real advection of ice particles to the coast by the surface velocities will even take longer because generally the ice will not be flowing the direct path assumed here.

References

Alyeska Pipeline Service Company: FACTS, Trans Alaska Pipeline System, Anchorage, Alaska. [online] Available from: www.alyeska-pipe.com, 2013.

Archer, C. L. and Jacobson, M. Z.: Evaluation of global wind power, J. Geophys. Res., 110(D12), 1–20, doi:10.1029/2004JD005462, 2005.

Bindschadler, R., Choi, H. and ASAID Collaborators: High-resolution Image-derived Grounding and Hydrostatic Lines for the Antarctic Ice Sheet, Boulder, Colorado, USA. [online] Available from: http://dx.doi.org/10.7265/N56T0JK2, 2011.

ECMWF: ERA-Interim, 2015 [online] Available from: http://apps.ecmwf.int/datasets/data/interim-full-daily/, n.d.

Fretwell, P., Pritchard, H. D., Vaughan, D. G., Bamber, J. L., Barrand, N. E., Bell, R., Bianchi, C., Bingham, R. G., Blankenship, D. D., Casassa, G., Catania, G., Callens, D., Conway, H., Cook, A. J., Corr, H. F. J., Damaske, D., Damm, V., Ferraccioli, F., Forsberg, R., Fujita, S., Gim, Y., Gogineni, P., Griggs, J. A., Hindmarsh, R. C. A., Holmlund, P., Holt, J. W., Jacobel, R. W., Jenkins, A., Jokat, W., Jordan, T., King, E. C., Kohler, J., Krabill, W., Riger-Kusk, M., Langley, K. A., Leitchenkov, G., Leuschen, C., Luyendyk, B. P., Matsuoka, K., Mouginot, J., Nitsche, F. O., Nogi, Y., Nost, O. A., Popov, S. V., Rignot, E., Rippin, D. M., Rivera, A., Roberts, J., Ross, N., Siegert, M. J., Smith, A. M., Steinhage, D., Studinger, M., Sun, B., Tinto, B. K., Welch, B. C., Wilson, D., Young, D. A., Xiangbin, C. and Zirizzotti, A.: Bedmap2: improved ice bed, surface and thickness datasets for Antarctica, Cryosph., 7, 375–393, doi:doi:10.5194/tc-7-375-2013, 2013.

Hinkel, J., Lincke, D., Vafeidis, A. T., Perrette, M., Nicholls, R. J., Tol, R. S. J., Marzeion, B., Fettweis, X., Ionescu, C. and Levermann, A.: Coastal flood damages and adaptation costs under 21st century sea-level rise, PNAS, 111(9), 3292–3297, 2014.

Marzeion, B. and Levermann, A.: Loss of cultural world heritage and currently inhabited places to sea-level rise, Environ. Res. Lett., 9(3), 034001, doi:10.1088/1748-9326/9/3/034001, 2014.

Melgarejo Moreno, Joaquín Sanz Montaño, B.: La eficiencia energética del trasvase Tajo-Segura, in Cuaderno Interdisciplinar de Desarrollo Sostenible, p. 174., 2009.

Rignot, E., Mouginot, J. and Scheuchl, B.: Ice flow of the Antarctic ice sheet." Science 333.6048 (2011): 1427-1430., Science (80-.)., 333(6048), 1427–1430, 2011.